# Polymer-Based 1 × 6 Thermooptic Switch Incorporating an Elliptic TIR Waveguide Mirror

Chiou-Hung Jang and Ray T. Chen

***Abstract*—A polymeric 1 × 6 thermooptic switch is fabricated and demonstrated. The device utilizes an elliptic total internal reflection waveguide mirror imaging the input channel waveguide onto the first output channel waveguide and a prism-array heating electrode steering the beam to corresponding output channel waveguides. At 1310 nm, 1 × 6 switching was demonstrated; the extinction ratios and crosstalks were found to be >20 and −20 dB, respectively. Switching time as low as 4 ms was observed. The device offers the advantage of single-electrode driving scheme for 1 × N(N > 2) switching.**

***Index Terms*—Beam steering, elliptic mirror, fiber switch, prism-array electrode, thermooptic, total internal reflection (TIR).**

## I. Introduction

THERE have been continuing needs to reduce cost and size while improving the performance of fiber-optic switches in communications, control, and metrology of optical instruments. Various approaches have been introduced, such as micromachined fiber-optic mechanical switches [1], [2] and electrical-mechanical switches [3]. However, these approaches suffered from problems such as low switching speed, high fabrication cost, and poor reliability due to the involvement of the moving components. Another method using electrooptic (EO) effect in waveguides [4]–[9] is attractive due to its high-speed capability. However, these devices are generally polarization sensitive and of high cost. On the other hand, realization of multiple (>2) switching channels has generally resorted to cascading multiple 1 × 2 or 2 × 2 switches [9]–[13], which requires multiple driving electrodes and therefore needs a very complex driving scheme.

Thermooptic (TO) effect in polymer has been an attractive approach for low-power operation due to its large TO coefficient ($\sim -10^{-4}/^{\circ}\mathrm{C}$) while on the other hand providing moderate response time, polarization-insensitive refractive index tuning, and low-cost fabrication. Our previous works [14], [15] have successfully demonstrated the beam steering capability of the prism-array electrode using TO effect.

In this paper, we shall describe the device concept, fabrication, experimental results, and analysis of a 1 × 6 fiber switch, which incorporates a prism-array electrode with an elliptic total internal reflection (TIR) waveguide mirror. The mirror provides the image mechanism mapping the input channel waveguide onto the designated channel waveguide, and the electrode steers the beam onto corresponding output channel waveguides. The device offers a simplified driving scheme for 1 × 6 switching.

Manuscript received July 9, 2002; revised December 5, 2002.

C.-H. Jang is with Intel Corporation, Hillsboro, OR 97124 USA.

R. T. Chen is with the Microelectronics Research Center, University of Texas at Austin, Austin, TX 78758 USA (e-mail: raychen@uts.cc.utexas.edu).

Digital Object Identifier 10.1109/JLT.2003.810089

## II. Device Design

Fig. 1 shows the schematic view of the device. The input channel and output channel #1 are placed at the two focal points of the elliptic TIR mirror, respectively. To image the input channel onto channel #1, the focal length $(f)$ of the mirror is designed to be far greater than Rayleigh range defined by the channel waveguide mode radius using Gaussian beam approximation [16]. That is

$$f \gg \frac{n_{\mathrm{eff}}\pi\omega_i^2}{\lambda} \tag{1}$$

where $n_{\mathrm{eff}}$ is the guided mode effective index, $\lambda$ is the wavelength, and $\omega_i$ is the mode radius. Note that the equation is modified by a factor of $n_{\mathrm{eff}}$ since the beam propagates in a waveguide. Employment of the elliptic TIR mirror as the imaging mechanism offers advantages such as focal length insensitive to material refractive index, small off-axis aberration, no mode mismatch at the mirror interface, and single step fabrication when compared with the waveguide lens approach [17]. These advantages help ease fabrication stringency and complexity.

A TO prism array electrode is placed along the way where the beam is being focused to steer the beam. To design a prism-array deflector with height large enough to retain the deflected beam inside the prism array while effectively keeping the deflection capability (smaller prism height gives rise to higher deflection capability), the most effective way is to have the light trajectory $x(z)$ parallel to the contour of the prism array $h(z)$ at its maximal deflection [14]. We start with

$$\frac{dh(z)}{dz} = \left.\frac{dx(z)}{dz}\right| \Delta n_{\mathrm{eff}} = \Delta n_{\mathrm{eff,max}}. \tag{2}$$

From the equation in [18], differentiating the equation with respect to $z$, and multiplying $1/n_{\mathrm{eff}}$ since the wave propagates in a waveguide, we have

$$d\theta_{\mathrm{def}} = \frac{\Delta n_{\mathrm{eff}}}{n_{\mathrm{eff}}}\frac{dz}{h(z)} \tag{3}$$

where $\theta_{\mathrm{def}}$ is the deflection angle. By combining (2) and (3) and the fact that $((d^2x(z))/(dz^2)) = ((d\theta_{\mathrm{def}})/(dz))$, we derive

$$\frac{d^2h(z)}{d^2z} = \frac{\Delta n_{\mathrm{eff,max}}}{n_{\mathrm{eff}}}\frac{1}{h(z)}. \tag{4}$$

Since the beam is being focused, the equation is solved under the initial conditions of $h(0) = h_0$ and $dh(0)/dz = h'_0$, where $h_0$ is the beam size at the elliptic mirror and $h'_0$ is the slope

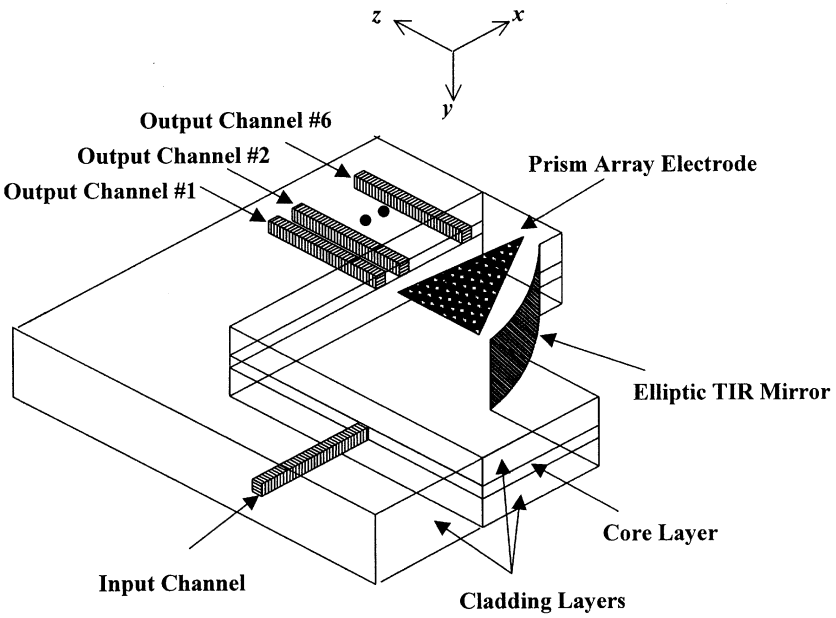


Fig. 1. Schematic view of the device.

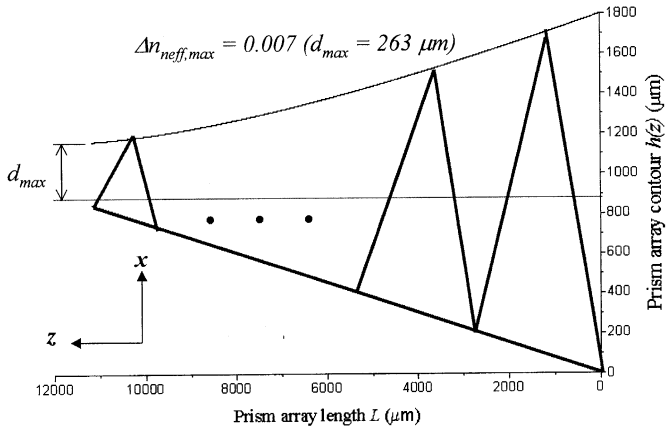


Fig. 2. Calculated prism array contour using $\Delta n_{\text{eff},max} = 0.007$, $f = 1.2$ cm, NA $= 0.12$, and $n_{\text{eff}} = 1.5$.

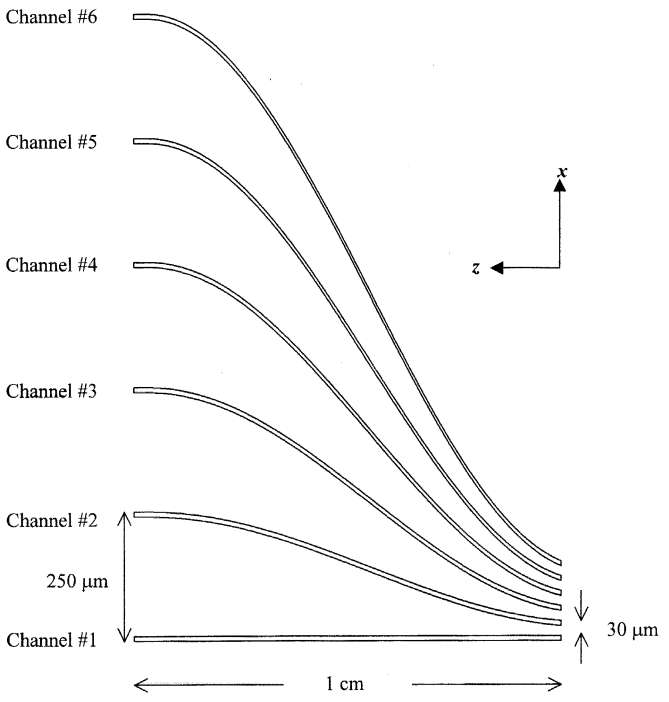


Fig. 3. Mask layout for the output fanout waveguides. The channel length is not to scale.

of beam divergence, both of which are governed by the numerical aperture (NA) of the channel waveguide and the focal length of the mirror. Note that the effective index change $\Delta n_{\text{eff}} = \Delta T_{\text{eff}} \times (dn/dt)$, $\Delta T_{\text{eff}}$ is the effective temperature change, $dn/dt$ is the TO coefficient of the material, and $z$ is the beam propagation direction, as shown in Fig. 1. Fig. 2 shows the calculated prism array contour using the following conditions: $\Delta n_{\text{eff},max} = 0.007$, $f = 1.2$ cm, NA $= 0.12$, and $n_{\text{eff}} = 1.5$.

A six-channel fanout waveguide was designed to collect the steered beam. To achieve more channel switching, the six output channels except channel #1 are designed cosine-curved. Fig. 3 shows the mask layout for the fanout waveguide, in which between adjacent channels the initial separation and that at the other end are 30 and 250 $\mu$m, respectively. The channels are designed with initial tilt angles according to the deflection angles. The channel length is designed to be 1 cm. Despite the fact that channel #6 is the most curved channel, beam propagation method (BPM) simulation results showed that the bent loss was less than 1 dB.

## III. Fabrication

The devices were fabricated on silicon wafers as the substrate. Two ultraviolet (UV) curable resin-based polymers, UV 15 and UV 11-3 from MasterBond Inc., whose refractive indexes were measured to be 1.506 and 1.513, respectively, at 1.3 $\mu$m for both

polarizations, were employed as the cladding and core materials. The chosen polymers are suitable for single-mode waveguide formation and have similar etch rate during reative ion etch (RIE), which is important for elliptic TIR mirror formation. For the waveguide formation, UV 15 was first spin-coated on the substrate as the bottom cladding layer. UV 11-3 was then spin-coated as the core layer and patterned by RIE for channel waveguide formation. UV 15 was again spin-coated as the top cladding layer. For both cladding layers, UV 15 was applied twice due to the low viscosity of the polymer solutions. Fig. 4 shows the photograph of the device input-end face, in which the channel dimension is 4.5 ×8.0 $\mu$m and the total waveguide thickness is around 18 $\mu$m. After the waveguides were formed, RIE was again applied for the formation of the elliptic TIR mirror. The etch rate was found to be 0.13 $\mu$m/min.

A 2000-Å gold layer was then deposited by e-beam deposition and patterned as a prism array according to Fig. 2. Fig. 5 shows the photo of a fabricated device sample. Each prism was designed in a way shown in the inset of Fig. 5, in which the electrode line running back and forth forms the prism area. Note that the electrode line width was designed to be 30 $\mu$m and the separation between the electrode lines was designed to be 2 $\mu$m.

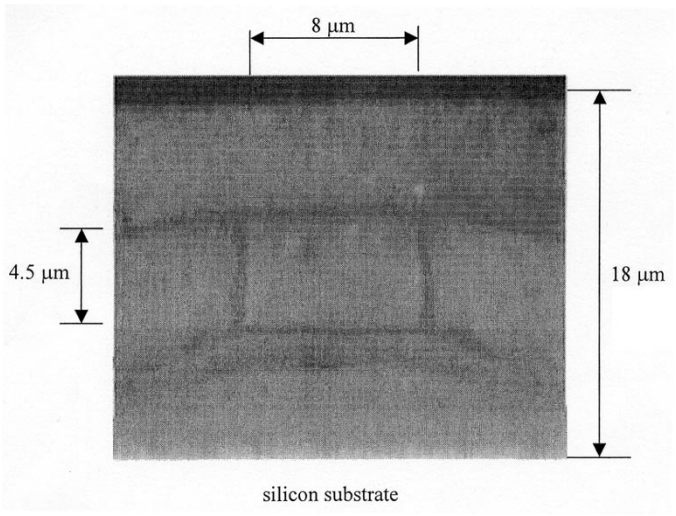


Fig. 4. Photograph of the device end face.

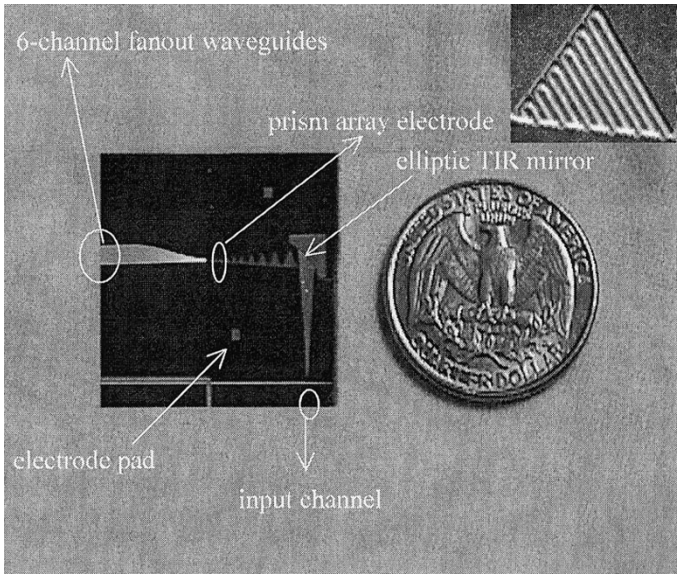


Fig. 5. Photograph of a fabricated device. The inset shows the magnification of a prism in the array.

## IV. Experiment and Discussion

To demonstrate the switching operation, a Nd:$YVO_4$ diode-pumped laser operating at 1310 nm was end-coupled into a single-mode fiber, which was butt-coupled with the input channel waveguide in the device. The input optical signal level was 20 mW (∼13 dBm). An eight-groove fiber array with 250-$\mu$m pitch was butt-coupled with the output channel waveguides and connected to a photodetector. A square-wave voltage signal with output voltage limit of 95 V was applied on the prism array electrode. Both the voltage signal and the optical signal from the photodetector were fed into an oscilloscope for comparison.

Fig. 6(a)–(f) shows the switching response from channel #1 to channel #6, respectively. The switching time was found to be 4 ms for channel #2 and increased to 7 ms for channel #6. The increase in switching time resulted from the time delay observed at the rising edges of the optical signals in channel #3 and on, which was considered due to the relatively large heating area. At zero applied voltage, the signal at channel #1 was −24 dBm, while ≤ −44 dBm for all other channels, giving a crosstalk of −20 dB. At 30 V, the signal level in channel #1 reduces from −24 to −55 dBm, giving an extinction ratio of 31 dB. However, the optical signal was not completely shifted to channel #2 at 30 V, indicating that the 30-$\mu$m initial channel separation was overly generous. At 36 V, the optical signal was completely shifted to channel #2 with the signal level increasing from −54 dBm to −22 dBm, giving the extinction ratio of 32 dB. We note that a 2-dB higher optical signal was observed in channel #2 than in channel #1, suggesting there might be a slight off targeting of the focused beam on channel #1 at zero applied voltage. The applied voltage $(V)$, corresponding power $(P)$, and optical signal level change in each channel are summarized in Table I.

The crosstalks were all found to be −20 dB when the beam was switched to different output channels, indicating that the focused spot size was not significantly enlarged due to beam deflection.

The time during which the optical signal held in a certain switched state was found to decrease as the applied electrical power $(P)$ increased. For switching to channel #2, the optical signal stayed stable for over 5 min without significant variation. However, for switching to channel #6, the optical signal drifted out of the channel, causing the signal level to decrease by 1 dB in around 10 s, showing that the corresponding $\Delta n_{\text{eff}}$ gradually increased. This could be attributed to the continuous accumulation of heat field inside the waveguide at high $P$, which implied the temperature increase in the substrate $\Delta T_{\text{sub}}$. The effect of the substrate thermal expansion $(\alpha_{\text{sub}})$ due to $\Delta T_{\text{sub}}$ *on* $\Delta n_{\text{eff}}$ could be significant in a three-dimensional channel waveguide; however, the effect was considered insignificant in

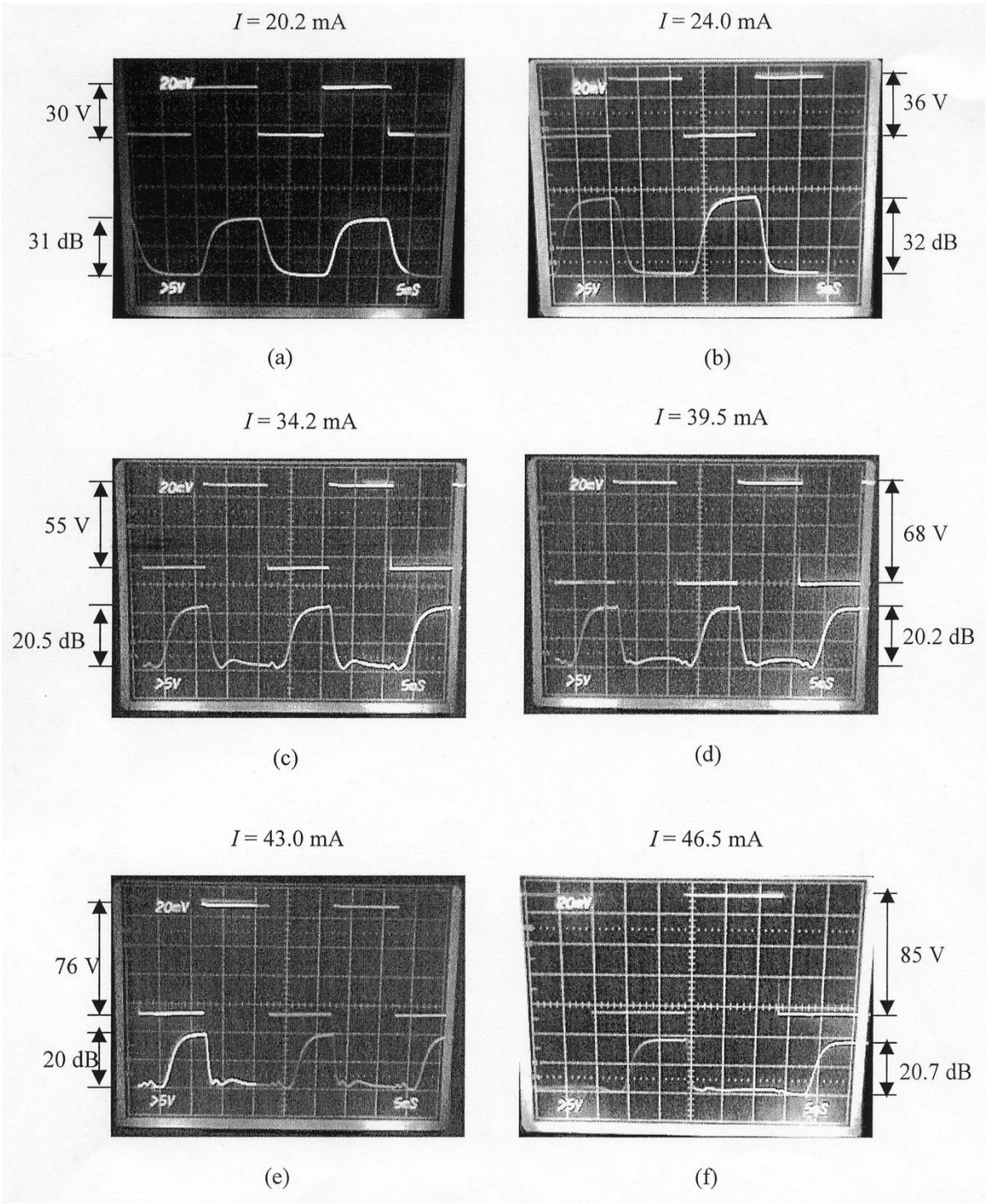


Fig. 6. The electrical signal (upper trace) and switching response (lower trace) in an oscilloscope for (a) channel #1, (b) channel #2, (c) channel #3, (d) channel #4, (e) channel #5, and (f) channel #6. The time scale is 5 ms/div.

our case since along the prism-array heating region, the guided wave propagated in a planar waveguide, whose temperature dependence $\Delta n_{\text{eff}}$ is theoretically independent of $\alpha_{\text{sub}}$ [19].

To determine electrode surface temperature change $(\Delta T_s)$ generated by $P$, we first found the relation between the electrode resistance $(R)$ and $P$

$$R = R_0 + C_p \times P \tag{5}$$

where $R_0$ is the electrode resistance at room temperature. $C_p$ was found to be 0.102 $\Omega$/mW. Secondly, we placed the electrode with the substrate on a hot plate to measure the temperature coefficient $(\alpha)$ of the electrode resistance. We found $\alpha = \Delta R/R_0/\Delta T_s = 3.1 \times 10^{-3}/^{\circ}\text{C}$. By combining the two relations, we have

$$\Delta T_s = \frac{C_p}{\alpha R_0} P. \tag{6}$$

TABLE I
SUMMARY OF APPLIED VOLTAGE, CORRESPONDING POWER, AND EXTINCTION RATIO FOR EACH OUTPUT CHANNEL

| Channel | #1 | #2 | #3 | #4 | #5 | #6 |
|---|---|---|---|---|---|---|
| $V$ (volt) | 30 | 36 | 55 | 68 | 76 | 85 |
| $P$ (mW) | 606 | 864 | 1881 | 2686 | 3268 | 3950 |
| Signal level change | from -24 dBm to -55 dBm | from -54 dBm to -22 dBm | from - 44 dBm to - 23.5 dBm | from - 44 dBm to - 23.8 dBm | from - 44 dBm to - 24 dBm | from -45 dBm to - 24.3 dBm |

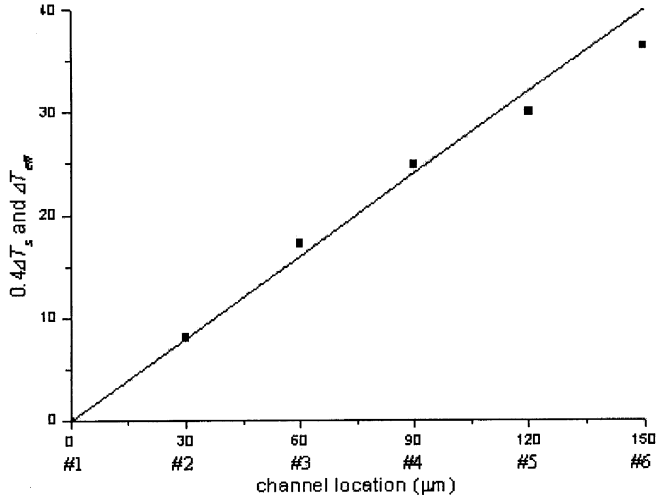


Fig. 7. Electrode surface temperature change ($\Delta T_s$) for corresponding channel: ($\Delta T_s$) is scaled by a factor of 0.4. The linear curve shows the calculation results of effective temperature change ($\Delta T_{\text{eff}}$) with respect to beam displacement calculated by (2).

The coefficient $C_p/\alpha/R_0$ was found to be 0.023°C/mW. The linear curve in Fig. 7 shows the calculation of $\Delta T_{\text{eff}}$ with respective to beam displacement, calculated by (4) with assumption of $dn/dt = -10^{-4}/°\text{C}$ for both core and cladding polymers (typical TO coefficient value for polymers). $\Delta T_s$ for each output channel calculated by (6) was found to fit well with the linear curve if being scaled by a factor of 0.4, as shown in Fig. 6. The results show the expected linear dependence of beam displacement on $\Delta T_s$ and also indicate $\Delta T_{\text{eff}} \approx 0.4\Delta T_s$. The factor of 0.4 can be a more reasonable value of 0.5 if we assume $dn/dt = -0.8 \times 10^{-4}/°\text{C}$, indicating that the chosen polymers might have a somewhat lower TO coefficient than the typical value.

The overall insertion loss was found to be 35 dB. An effort was made to measure the material absorption of the core-layer polymer UV 11-3. At 1300 nm, an optical transmittance of 97.3% over a $\sim 127 - \mu$m UV 11-3 film was measured, the corresponding loss was 9.36 dB/cm. With the device length of around 3.5 cm, the result suggested the overall insertion loss was primarily due to material absorption loss.

The polarization dependence of the device operation was examined using TE and TM polarized light separately to test the device. No significant difference was found in the device switching characteristics. Considering the device operation, despite the small difference in waveguiding characteristics between the two polarizations, the only polarization-dependent component—the dependence of phase shift upon the incident angle after TIR, also known as Goos–Hänchen shift—was found to be around 1.0 and 1.8 $\mu$m, respectively, for TM and TE polarizations in our case of 45° incident angle [20], which was considered negligible and explained the polarization-insensitive operation of the device.

## V. SUMMARY

A polymeric 1 × 6 fiber-optic switch using a thermooptic prism array electrode and an elliptic TIR waveguide mirror was fabricated and demonstrated. The device utilizes the elliptic waveguide mirror as the imaging mechanism and a TO prism array electrode as the beam steering mechanism for switching operation. The measured extinction ratios and applied electrical power were summarized in Table I. Crosstalk of −20 dB and switching time as low as 4 ms were observed, and the power consumption on average was 790 mW/channel. The overall insertion loss was considered primarily due to the material absorption loss. The device offers a single-electrode driving scheme for 1 × 6 switching.

## ACKNOWLEDGMENT

The authors would like to thank AFOSR, BMDO, and ONR for their support and the reviewers for their valuable comments.

## REFERENCES

[1] C. Gonzalez and S. D. Collins, "Micromachined 1 × n fiber-optic switch," *IEEE Photon. Technol. Lett.*, vol. 9, pp. 616–618, May 1997.
[2] R. T. Chen, H. Nguyen, and M. C. Wu, "A high-speed low-voltage stress-induced micromachined 2 × 2 optical switch," *IEEE Photon. Technol. Lett.*, vol. 11, pp. 1396–1398, Nov. 1999.
[3] M. Shimizu, K. Yoshida, and R. Ohta, "Mechanical optical switch for single-mode fiber," *IEICE Trans. Commun.*, vol. E76-B, no. 4, pp. 370–374, 1998.
[4] R. C. Alferness, "Waveguide electrooptic switch arrays," *IEEE J. Select. Areas Commun.*, vol. 6, pp. 1117–1130, Aug. 1988.

[5] R. M. Jenkins, J. M. Heaton, D. R. Wight, J. T. Parker, J. C. H. Birbeck, G. W. Smith, and K. P. Hilton, "Novel 1 × N and N × N integrated optical switches using self-imaging multimode GaAs/AIGaAs waveguides," *Appl. Phys. Lett.*, vol. 64, no. 6, pp. 684–686, 1994.
[6] J. I. Thackara, J. C. Chon, G. C. Bjorklund, W. Volksen, and D. M. Burland, "Polymeric electro-optic Mach–Zehnder switches," *Appl. Phys. Lett.*, vol. 67, no. 26, pp. 3874–3876, 1995.
[7] N. W. Rimington, A. I. Cornea, J. Santoro, T. R. Nelson, and W. A. Schroeder, "A multi-kilohertz electro-optic switch for ultrafast laser systems," in *Conf. Lasers Electro-Optics*, 2000, pp. 121–122.
[8] K. Nashimoto, H. Moriyama, S. Nakamura, M. Watanabe, T. Morikawa, E. Osakabe, and K. Haga, "PLZT electro-optic waveguides and switches," *Opt. Fiber Commun.Conf.*, vol. 4, pp. PD10-1–PD10-3, 2001.
[9] L. McCaughan and G. A. Bogert, "$4 \times 4$ $\mathrm{Ti:LiNbO_3}$ integrated-optical crossbar switch array," *Appl. Phys. Lett.*, vol. 47, no. 4, pp. 348–350, 1985.
[10] M. Schienle, G. Wenger, S. Eichinger, J. Muller, L. Stoll, and G. Muller, "A 1 × 8 InP/InGaAsP optical matrix switch with low insertion loss and high crosstalk suppression," *J. Lightwave Technol.*, vol. 14, pp. 822–826, May 1996.
[11] N. Keil, H. Yao, C. Zawadzki, K. Losch, K. Satzke, W. Wischmann, J. Wirth, J. Schneider, J. Bauer, and M. Bauer, "Thermo-optic 1 × 2- and 1 × 8-vertical coupled switches (VCS) using hybrid polymer/silica integration technology," in *OFC 2001*, vol. 3, 2001, pp. WR2-1–WR2-3.
[12] E. J. Murphy, C. T. Kemmerer, D. T. Moser, M. R. Serbin, J. E. Watson, and P. L. Stoddard, "Uniform 8 × 8 lithium niobate switch arrays," *J. Lightwave Technol.*, vol. 13, no. 5, pp. 967–970, 1995.
[13] T. Goh, M. Yasu, K. Hattori, A. Himeno, M. Okuno, and Y. Ohmori, "Low-loss and high-extinction-ratio silica-based strictly nonblocking 16 × 16 thermooptic matrix switch," *IEEE Photon. Technol. Lett.*, vol. 10, pp. 810–812, June 1998.
[14] C.-H. Jang, L. Sun, J.-H. Kim, X. Lu, G. Karve, R. T. Chen, and J. Maki, "A thin-film polymeric waveguide beam deflector based on thermooptic effect," *IEEE Photon. Technol. Lett.*, vol. 13, pp. 490–492, May 2001.
[15] J.-H. Kim, L. Sun, C.-H. Jang, C.-C. Choi, and R. T. Chen, "Polymeric waveguide thermooptic beam deflector with dual folded-thin-strip heating electrode," unpublished.
[16] B. E. A. Saleh and M. C. Teich, *Fundamentals of Photonics*. New York: Wiley, 1991, pp. 86–89.
[17] M. Minot and C. Lee, "A new guided-wave lens structure," *J. Lightwave Technol.*, vol. 8, pp. 1856–1865, Dec. 1990.
[18] Y. Yariv, *Introduction to Optical Electronics*. New York: Holt, Rinehart and Winston, 1976, p. 266.
[19] Y. Kokubun, N. Funato, and M. Takizawa, "Athermal waveguides for temperature-independent lightwave devices," *IEEE Photon. Technol. Lett.*, vol. 5, pp. 1297–1300, Nov. 1993.
[20] H. Nishihara, M. Haruna, and T. Suhara, *Optical Integrated Circuits*. New York: McGraw-Hill, 1989, p. 16.

**Chiou-Hung Jang** received the B.S. degree in physics from National Tsing Hua University, Taiwan, in 1995, the M.S. degree in electronics engineering from National Chiao Tung University, Taiwan, in 1997, and the Ph.D. degree in electrical and computer engineering from the University of Texas at Austin in 2002. His doctoral research focused on theoretical analysis, design/simulation, and implementation of fiber-optic switches.

He recently joined Intel Corporation for research and development on lithography enhancement.

**Ray T. Chen**, photograph and biography not available at the time of publication.